Article

Not peer-reviewed version

Innovations in Electrochemical Sensors for Lead Ion Detection: Applications in Wastewater Treatment and Cytotoxicity Assessment

Morris Kamel , Gehad Abd El-Fatah , Mohamed Zaky , Amal Zaher , Ahmed Farghali , Sarah I. Othman , Ahmed Allam , Hassan Ahmed Rudayni , Mohamed E. M. Hassouna , Rehab Mahmoud *

Posted Date: 19 October 2023

doi: 10.20944/preprints202310.1287.v1

Keywords: lead ions (Pb+2); Zn-Fe LDH/PANI; Carbon paste electrode (CPE); differential pulse voltammetry (DPV); Zn/Mg/Fe LDH; Atomic absorption spectrophotometer (ASS); cytotoxicity

Article

Innovations in Electrochemical Sensors for Lead Ion Detection: Applications in Wastewater Treatment and Cytotoxicity Assessment

Morris Kamel [1], Gehad Abd El-Fatah [1], Mohamed Y. Zaky [2], Amal Zaher [3], Ahmed A. Farghali [4], Sarah I. Othman [5], Ahmed A. Allam [6], Hassan Ahmed Rudayni [7], Mohamed E. M. Hassouna [1,*] and Rehab Mahmoud [1]

[1] Department of Chemistry, Faculty of Science, Beni-Suef University, 62511 Beni-Suef, Egypt.
[2] Molecular Physiology Division, Zoology Department, Faculty of Science, Beni-Suef University, Beni-Suef, Egypt
[3] Environmental Science and Industrial Development Department, Faculty of Postgraduate Studies for Advanced Sciences, Beni-Suef University, 62511 Beni-Suef, Egypt.
[4] Materials Science and Nanotechnology Department, Faculty of Postgraduate Studies for Advanced Sciences, Beni-Suef University, Beni-Suef, Egypt.
[5] Department of Biology, college of Science, Princess Nourah bint Abdulrahman University, P.O. BOX 84428, Riyadh 11671.
[6] Department of Zoology, Faculty of Science, Beni-suef University, Beni-suef 65211 Egypt.
[7] Department of Biology, College of Science, Imam Muhammad bin Saud Islamic University, Riyadh 11623, Saudi Arabia.

Abstract: The requirement for developing tools capable of detecting and monitoring heavy metals (HMs) has recently taken on more significance due to worries about their toxic effect on human health and aquatic habitats. In this study, a simple electrochemical sensing carbon paste electrode (CPE) based on composite of Zinc/Iron layered double hydroxide (LDH) and polyaniline (PANI) was developed for the determination of lead ions in aquatic solutions. For this purpose, Zn-Fe LDH/PANI was prepared and characterized by Fourier-transform infrared (FTIR), X-ray diffraction (XRD), and scanning electron microscopy (SEM). Modified carbon electrode based Zn-Fe LDH/PANI was electrochemically characterized compared with unmodified electrode in FCN as a redox probe using cyclic voltammetry (CV). Thus, Zn-Fe LDH/PANI was utilized as sensing material for the electrochemical determination of lead ions using differential pulse voltammetry (DPV). Zn-Fe LDH/PANI/CPE show limits of detection (LOD) and quantification (LOQ) of 167.8 nM and 559.4 nM, respectively. Zn/Mg/Fe LDH was prepared using co-precipitation method and characterized by XRD, FTIR, SEM and BET, used for removal of Pb^{+2} ions. Removal process was investigated at different conditions as pH, metal ion concentrations, starting adsorbent dose at first and contact time. Zn/Mg/Fe LDH was evaluated as an effective adsorbent material for lead ions elimination in aquatic solutions, with capacity of adsorption 700 mg/g. The elimination of lead ions on Zn/Mg/Fe LDH fitted the pseudo first-order kinetics model and the isotherm was matched with Langmuir model. Studies revealed that the ideal removal conditions were pH = 5.0, an adsorbent mass of 0.05 g, and 20 ml of 50 ppm metal ion concentration at 60 min. The Zn-Fe LDH/PANI composite also showed potential anti-cancer properties against lung cancer cells (A549) while maintaining safety for normal lung fibroblast cells (WI-38). Collectively, advancements in electrochemical sensors offer promising solutions for lead ion detection, with wide-reaching applications in wastewater treatment and cytotoxicity assessment. These innovations have the potential to enhance environmental monitoring and public health safety.

Keywords: lead ions (Pb^{+2}); Zn-Fe LDH/PANI; Carbon paste electrode (CPE); differential pulse voltammetry (DPV); Zn/Mg/Fe LDH; Atomic absorption spectrophotometer (ASS); cytotoxicity

1. Introduction:

Preprints (www.preprints.org) | NOT PEER-REVIEWED | Posted: 19 October 2023 doi:10.20944/preprints202310.1287.v1

Heavy metals are a significant environmental issue because they are both not biodegradable and extremely poisonous to all living organisms [1–4]. As a result, these hazardous elements permanently endanger both human health and aquatic ecosystems [5,6]. Even at low concentrations, exposure can have immediate and long-term consequences for human health. Lead is considered one of the most toxic HMs and has a serious bad effect on human health and the aquatic system. Lead pollution is mostly caused by the manufacturing of PVC pipes used in agriculture and sanitary systems, as well as by lead batteries and lunch boxes[7]. Exposure to lead in humans causes haematological, neurological, and renal side effects, including developmental and behavioral problems in young children, inhibition of haemoglobin synthesis, and kidney disease or hyperuricemia [8]. The World Health Organization (WHO) has advised that the concentration of Pb^{2+} ions in drinking water must be bellower than 10 nM [9]. Thus, the precise and sensitive detection of traces of Pb^{+2} ions, has emerged as a key concern and challenge for the scientific community in light of these harmful implications for human health and the environment. A set of spectrometric ways have been used to achieve this purpose, including atomic absorption spectrometry, inductively coupled plasma atomic spectrometry, mass spectrometry, and X-ray fluorescence spectrometry[10,11]. Despite the fact that most of these methods require expensive equipment, long time for sample preparing and analysis steps [12]. As a consequence, the evolution of electrochemical platforms based on developed electrodes has been encouraged by the use of electrochemical methods as alternatives. Nonetheless, these techniques use simple, low-cost equipment and are less time-consuming. The DPV approach is one of the electrochemical methods used for precise, sensitive, and low detection limit measurement of species [13]. Chemically evaluated carbon paste electrodes were employed recently to enhance the sensitivity, selectivity and detection limit. For instance, many materials have been utilized as modifiers inside the electrode structure [14]. More intriguingly, when the material of the electrode is easily chosen to exhibit chemical affinity for the target analyte, they are sensitive and selective [15]. Since nanomaterials have a large surface area, an electrode that has been modified by nanomaterials performs better in terms of selectivity, stability, and sensitivity [16,17]. A very active field of research is the modification of the sensing platforms by organic conducting polymers. The potential use of organic conducting polymers as electrochemical sensors attracted a lot of attention[18,19]. In addition, removing the process of Pb^{+2} ions from wastewater is of utmost importance to maintain environmental standards and for human health [20]. LDHs are now used in waste water treatment techniques [21,22], they are anionic clays with two-dimensional nanostructures. The lamellar structure of LDHs is composed of layers carry positive charges that resemble sheets with anion-intercalated and molecules of water. LDHs are a significant and effective adsorbent for many contaminants because they have large surface area and high anion exchange capacity [23]. Low cost, easy preparation, and high efficiency make LDHs a good adsorbent for the removal of HMs; Table 1 shows removal capacities for different LDHs.

In this present work, we constructed a sensitive platform for electrochemical determination of lead ions in aquatic solutions using DPV technique. Besides, the direct application of LDHs was prepared by the co-precipitation way for the elimination of lead ions under different experimental conditions (pH, pollutant concentration, adsorbent dose, and time).

Table 1. Comparing the removal of Pb^{2+} ions by various adsorbents adsorption capacities (q_m).

Adsorbent	Q_{max} (mg/g)	pH	Conc. (mg/l)	Ref.
Mg/Al LDH	3.20	2-4	40	Yamin Yasin et al 2013 [24]
Co/Mo LDH	73.40	5.5	370	Mohsen S.Mostafa 2016 [25]
Mg/Fe intercalated with local adsorbent	26.24	5.0	500	Abdul Hameed et al 2020 [26]
Citrate modified Mg/Al	298.50	6.0		Weigiangchen et al 2017 [27]

 doi:10.20944/preprints202310.1287.v1

chitosan/Mg-Al LDH	333.30	5.0-7.0	300	Feiyanlyu 2018 [28]
magnetic alginate microsphere based on Fe_3O_4 /MgAl LDH	266.60	5.0-6.0	400	Junhao Sun 2018 [29]
Mg_2Al–LS–LDH (Sulfonated lignin)	123.00	5.7 -5.8	200	Gailing Huang [30]
Zn/Mg/Fe LDH	700.00	5.0	50	current study

2. Experimental

2.1. Chemicals and reagents

The nitrates used in this latest study were obtained from Alpha Chemika (Egypt) and included lead nitrate $Pb(NO_3)_2$, zinc nitrate $Zn(NO_3)_2.6H_2O$, ferric nitrate $Fe(NO_3)_3.9H_2O$, and magnesium nitrate $Mg(NO_3)_2.6H_2O$. Hydrochloric acid (HCl) and sodium hydroxide (NaOH) were acquired from Carloerba Reagents (Egypt) and Piochem for laboratory chemicals in Egypt, respectively. Chloroform, aniline, and ammonium persulfate (APS) were brought from Laboratory Chemicals Reagents, Fine Chemicals, for the creation of polyaniline (PANI). All substances and reagents are of high analytical grade. For the manufacture of carbon electrodes, paraffin oil and graphite powder were provided by Alpha Chemika. N, N dimethyl formamide (DMF) was provided by Fisher Chemicals. For electrochemical characterization of carbon electrodes, potassium ferricyanide and potassium ferrocyanide were acquired from Piochem and alpha chemika, respectively. Used electrolytes were prepared using deionized water (DI), including nitric acid (HNO_3) and potassium chloride (KCl).

2.2. Synthesis of Zn/Fe LDH/ PANI

First, Zn/Fe-layered double hydroxide was prepared using the previously described co-precipitation technique [31]. Zn-Fe LDH/PANI was created by mixing 0.50 g of the obtained Zn/Fe LDH in 20 ml of chloroform with constant stirring for 1 h, followed by adding 0.05 M of aniline. Another prepared solution of 0.050 M potassium persulfate in 20.0 ml (0.10 M) HCl was added to the Zn/Fe LDH and aniline mixture with stirring and left until a black-green precipitate formed. The resultant precipitate was washed many times with DI and then dried for 24 hours at 60 °C.

2.3. Carbon paste electrodes preparation

Carbon paste electrodes were constructed by mixing 0.50 g of graphite powder with 0.10 ml of paraffin oil, packing the mixture into a Teflon tube as a holder, and connecting the tube with a copper wire. The electrode surface was glazed in order to produce a glossy electrode surface. Zn/Fe LDH-PANI/CPE was prepared by combining 1.0 ml of DMF with 6 mg of Zn/Fe LDH-PANI and sonicating the mixture for two hours. 20.0 µL of the mixture was added drop wise on the surface of the electrode and dried in an oven at 40 °C for 20 min. Before usage, the prepared electrodes were rinsed with DI.

2.4. Preparation of Zn/Mg/Fe LDH

A simple co-precipitation technique was used to create Zn/Mg/Fe LDH with a molar ratio of 4:4:1. Zinc nitrate, magnesium nitrate, and iron nitrate were dissolved in 200 ml DI. NaOH solution (2M) was added dropwise at a very slow rate until the pH level at 25 ˚C reached 10. After 24 hours of stirring, the precipitate was recovered by centrifugation, repeatedly washed with DI to remove any

 doi:10.20944/preprints202310.1287.v1

remaining base, until the pH reached 7, and then dried at 80 ℃ overnight. After that, the Zn/Mg/Fe LDH was grinded to a uniform particle size.

2.5. Equipments and instruments

A potentiostat or galvanostat (AUTOLAB PGSTAT 302N, Metrohm, Utrecht, and the Netherlands) was employed to conduct the electrochemical measurements. The working electrode is a modified carbon electrode, the reference electrode is Ag/AgCl, and the counter electrode is platinum wire (Pt). The electrochemical cell is connected to these three electrodes. The produced materials were examined using an FTIR spectrometer with a broker (vertex 70 FT-IR) analyzer in the range of 4000 to 400 cm-1 (Germany), Cu Ka radiation at a wavelength of 0.154 cm-1 was utilized to determine the patterns of XRD using a PAN analytical (empyrean) X-ray diffraction system in the United Kingdom at an accelerating voltage of 40 kv, current of 35 mA, scan angle 5-75° range, and scan step 0.02. JEOL-JEM 2100 (Japan) and Quanta FEG 250 (Switzerland) both have an acceleration voltage of 200 Kv. To examine the fabricated materials' microstructures and describe solid morphologies, FESEM micrographs were captured. The Braeur-Emmett-Teller (BET) specific surface area, pore size, and specific pore volumes of the (Zn/Mg/Fe LDH) were determined using Quantachrometouchwin TM version 1.21. Agilent Technologies 240FS AA atomic absorption spectrometer was used to measure the concentration of lead ions in the sample. Adwa-AD 1030 pH meter was used to determine the solution's pH.

2.6. Electrochemical examinations

Zn-Fe LDH/PANI was used as the improved sensing compound for the carbon paste electrode in the voltammetric tests for the detection of Pb^{+2} ions. The measurement of Pb^{+2} ions in 0.1 M HNO3 with a pH value of 2 as the supporting electrolyte was carried out using differential pulse voltammetry (DPV). Using Zn-Fe LDH/PANI/CPE, the electrochemical measurements for Pb^{+2} ions were performed at a deposition potential of -0.8V and a potential range of 0.8 V to 0.1 V.

2.7. Adsorption studies

range of concentrations that were then combined with Zn/Mg/Fe LDH at 200 rpm on a shaker for 24 hours at room temperature. All tests were carried out using this procedure. The influence of pH (from 3 to 6) for a solution using 0.1M NaOH and 0.1M HCl using a pH-meter, varied time intervals (5 to 120 min), the dose of adsorbent, and beginning metal ion concentration were among the several adsorption conditions that were examined. After centrifuging the adsorbent to remove impurities, the concentration of lead was measured using an atomic adsorption spectrometer (Agilent Technologies 240FS AA), applying the mass balance equation, the quantity of lead uptake at equilibrium qe (mg/g) was calculated. (1)[32–34]

$$q_e = \frac{V(C_\circ - Ce)}{m} \qquad (1)$$

Where, q_e (mg/g) is equilibrium adsorption capacity, $C_\circ$ and C_e (mg/l) represents concentration and equilibrium concentration of Pb^{2+}, m is the adsorbent mass, V is solution volume (L).

According to equation (2), the adsorption efficiency (Q %) of lead in the Zn/Mg/Fe LDH was calculated

$$Q\% = \frac{C_\circ - Ct}{C_\circ} \times 100 \qquad (2)$$

where C_t represents Pb^{2+} concentration after adsorption time t

Different initial concentrations of Pb^{2+} were used ranging from 5 mg/L to 100 mg/L to study the adsorption isotherms. Moreover, numerous isotherm models have been performed to fit the adsorption data. Pb^{2+} adsorption kinetics were studied and then applyed to various kinetic models such as pseudo-first-order, pseudo-second-order, intra-particle diffusion, and Avrami.

 doi:10.20944/preprints202310.1287.v1

2.8. Cell culture

Egypt's Holding Company for Biological Products and Vaccines (VACSERA) supplied the research with human lung cancer cells (A549) and the human normal lung fibroblast cell line (WI-38). A549 cells were grown in RPMI 1640 medium (from Gibco, San Jose, CA, USA), while WI-38 cells were cultured in DMEM medium (also from Gibco, San Jose, CA, USA), supplemented with 10% fetal bovine serum. These cells were incubated at 37°C in a humidified incubator with 5% CO2.

2.9. MTT assay

A549 and WI-38 cells were seeded in 96-well plates at a density of 1.5×10^6 cells per well. After 24 hours, these cells were exposed to varying concentrations of Zn-Fe LDH/PANI, specifically 100, 50, 25, 12.5, and 6.25µg/mL. Control cells were treated with DMSO. Subsequently, 3-(4,5-dimethylthiazol-2-yl)-2,5-diphenyltetrazolium bromide (MTT) was added to each well and incubated for an additional 2 h after 48 h of drug treatment. The resulting formazan was dissolved in DMSO, and the optical density (OD) at 590 nm was measured to calculate the percentage cell viability using a Sunrise microplate reader from TECAN, Inc. (USA).

3. Results and data analysis

3.1. Investigation of Zn/Fe LDH/PANI

Zn/Fe LDH/PANI was synthesized and investigated by SEM, FTIR and XRD. In order to determine the vibration of chemical bonds, FTIR spectra were obtained for the prepared material in the 500-4000 cm^{-1} range as represented in Figure 1(a). A strong peak at 1117 cm-1 was discovered, which was attributed to PANI C - C stretching. The band at 3425 cm-1 was caused by the overlap of N-H stretching vibrations of PANI and -OH stretching vibrations of hydroxyl groups on LDH layers. Peaks in the 800-500 cm1 range were observed as a result of the stretching and bending vibrations of Fe-O bonds and Zn-O bonds. The faint peak at 2918 cm^{-1} represented the stretching of $-CH_2-$ groups in PANI. The stretching of C=C in PANI rings was observed at 1570 cm^{-1}. The peak observed at 1307 cm^{-1} represented the vibration stretching of NO_3^- anions in the layers of LDH.

XRD analysis was performed for purity, atomic structure, and crystallite investigation. XRD was performed at of 10^o to 80^o range as represented in Figure 1 (b). The morphology of Zn/Fe LDH/PANI was defined by SEM as shown in Figure 1 (c). From the Figure 1(c) we can see the particles appeared as spheres and network structures, particles with average sizes of 36-58 nm. Many pores were observed in Figure 1(c), this porosity increases the process of adsorption on the nanostructure's surface.

Preprints (www.preprints.org) | NOT PEER-REVIEWED | Posted: 19 October 2023 doi:10.20944/preprints202310.1287.v1

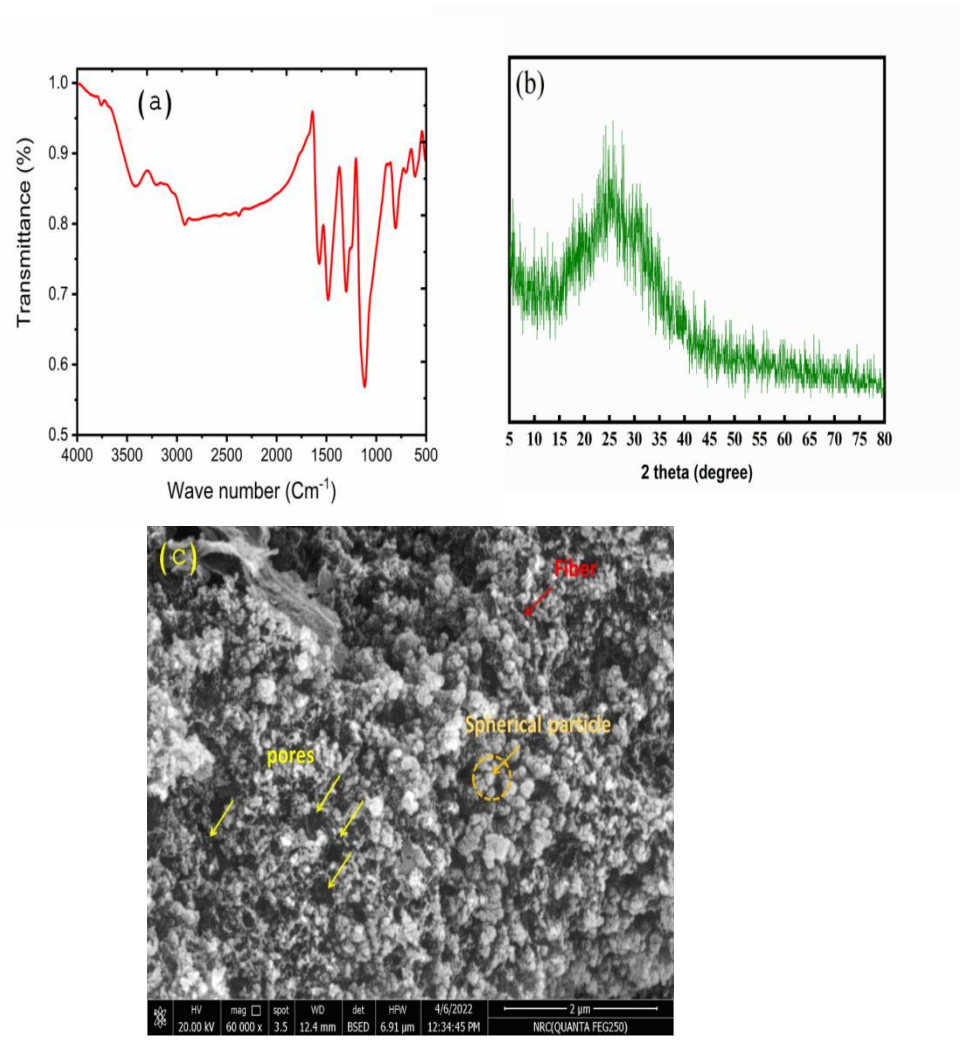

Figure 1. FT-IR (a); XRD (b) and SEM image (c) of Zn-Fe LDH/PANI.

3.2. Characterization of the Zn/ Mg/Fe LDH.

Figure 2(a) shows the Fourier transform infrared (FT-IR) spectrum of LDH. According to Fig 2(a), the strong broad band at 3415.44 cm-1 in these spectra may be caused by the existence of O-H stretching vibrations of the physically adsorbed water molecules and the hydrogen bonding - OH interlayer groups, which are discernible in the LDH's FTIR spectra. While the hydroxyl group's bending vibration may be seen at a wavelength of 1631.6 cm-1. Referring to the asymmetric stretching vibration of NO_3 anions in the LDH interlayer, the peak is situated at 1380.40 cm-1. The stretching vibrations of M-O and M-O-H in Figure 2(a) may be the cause of the peaks at 695 cm-1 and 460.77 cm-1.

Figure 2(b) shows the XRD pattern for the adsorbent (LDH), which is a typical reflection of the LDH. There are peaks at 2θ of 60º, 34º, 22º and 11º which correspond to ((011), (009), (006), and (003), respectively, The XRD chart proposed the production of crystalline LDH (Figure 2(b)). The basal spacing for the highest peak intensity, 2=34º, is 2.6361 for the largest peak. Applying Deby-Sherrer's equation [36], the Mg/Zn/Fe LDH crystals size was calculated to be 9.9 nm.

SEM was used to study the prepared LDH´s morphology. SEM photo shows a layer´s structure (Figure 2(c-d)), which is common for layered double hydroxide nanomaterials. Also, the layers aggregate and form flower structure with high porosity in Figure 2(d) like a flower formed from a good compact layered structure of Zn/Mg/Fe LDH. Figure S1 displays the constructed LDH's N2 gas adsorption-desorption. These parameters influence the adsorption behavior of the synthesized LDH by measuring its surface area, mesoporosity, and average pore size. The isotherm of the adsorbent of type V is associated with the back loop of H4 and H3 type occurs when the adsorbent, particularly

Preprints (www.preprints.org) | NOT PEER-REVIEWED | Posted: 19 October 2023 doi:10.20944/preprints202310.1287.v1

the monolayer, interacts instead of the sample's surface, according to the IUPAC classification. This attitude can be caused by the creation of a weak bulk of plate-like shape particles or the clustering of crack-shaped pores. The BET surface area of the prepared LDH was 368.90 m^2/g, mean pore diameter 6.70 cm3/g and its total pore volume 0.62 nm. These values can give us confirmation that prepared LDH will be good adsorbent.

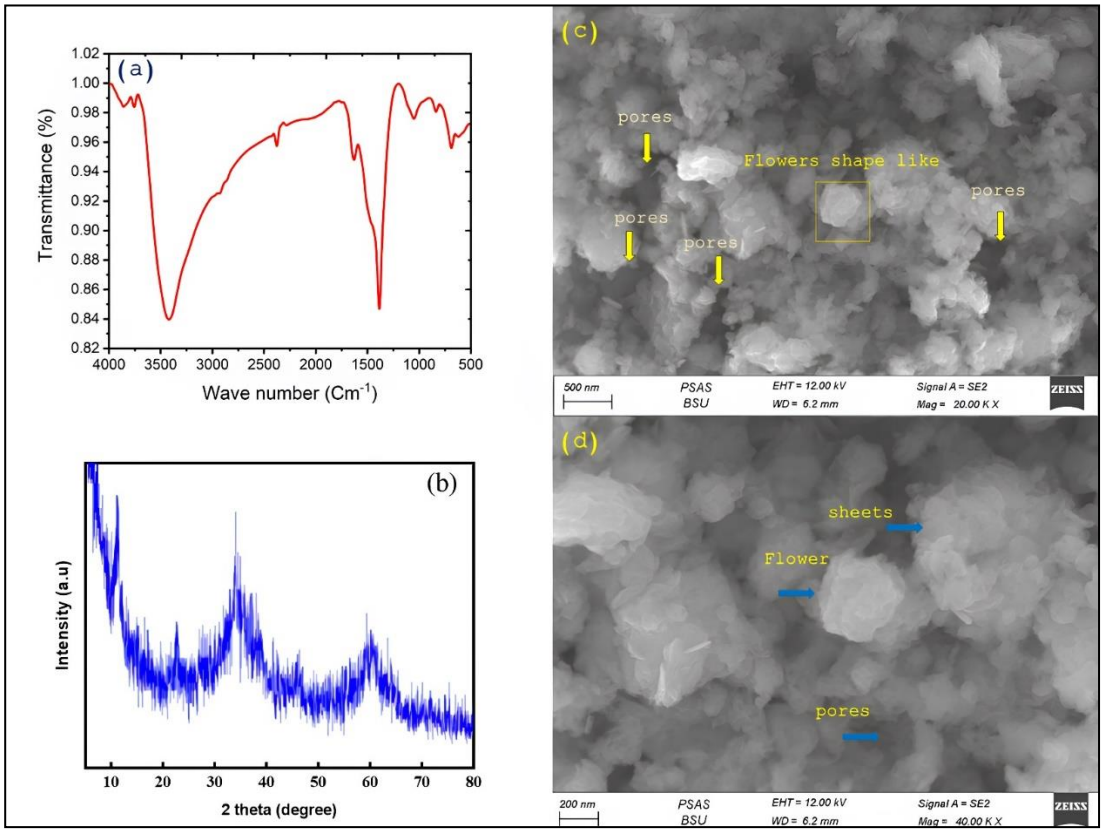

Figure 2. FT-IR spectra for (a); XRD patterns (b); SEM images (c-d) of the prepared Zn/Mg/Fe LDH.

3.3. Electrochemical characterization for the obtained Zn/Fe LDH/PANI/CPE

In this work, a modified carbon paste electrode with Zn/Fe LDH/PANI was used for the measuring of Pb^{+2}. A prepared electrode was electrochemically characterized in 0.10 M KCl containing 5.0 mM $K_3[Fe(CN)_6]^{3/4}$ with a Scan rate 0.050 V/S, step potential 0.01 V, equilibrium time 15.0 sec and potential range from - 0.40 V to 1.00 V. Modified platform with Zn-Fe LDH/PANI show high oxidation current compared to unmodified carbon paste electrodes, as shown in Figure 3(a).

3.4. Calibration curve

Nitric acid (HNO_3) with 0.10 M at pH 2.0 is used as a supporting electrolyte; a calibration curve was performed at deposition potential -0.8V, deposition time 30 s, step potential 0.01V, and equilibrium time 15 s. Sharp DPV peak was observed for the detection of Pb^{+2} ions, by increasing the concentration of lead ion the oxidation anodic current increased in Figure 3(b). The linear range was from 1 - 80 μM as represented in Figure 3(c). The (R^2) correlation coefficient was 0.973, and the corresponding linear equation was y = 4.73 x – 8.597. The limit detection (LOD) was 167.8 nM and the limit of quantification (LOQ) was 559.4 nM.

Preprints (www.preprints.org) | NOT PEER-REVIEWED | Posted: 19 October 2023 doi:10.20944/preprints202310.1287.v1

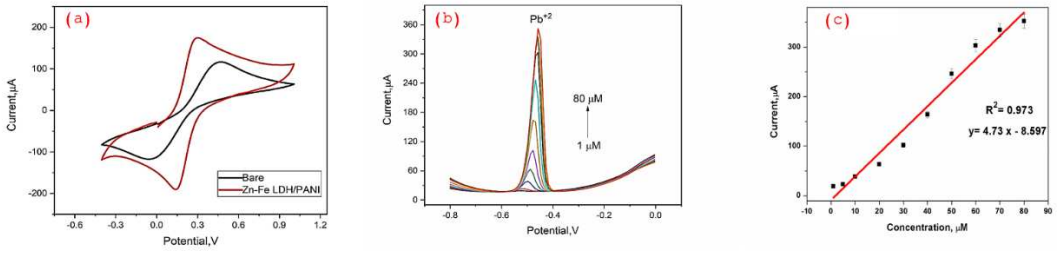

Figure 3. CV for carbon bare and modified CPE with Zn-Fe LDH/PANI in 0.10 M KCl containing 5.0 mM $K_3[Fe(CN)_6]^{3/4}$ (a); The DPV responses of the proposed sensor to various concentrations of Pb^{+2} ions in 0.1 M HNO3 at pH 2 (b) and a linear relationship between the concentration and related oxidation current values of Pb^{+2} ions (c).

3.5. Adsorption optimization parameters

3.5.1. The effect of medium pH on the elimination of Pb^{2+} metal ions

The effect of the pH of the solution on the elimination of Pb^{+2} from aquatic mediums using Zn/Mg/Fe LDH in the pH range of 3-7 with an initial Pb^{+2} concentration of 30 ppm was examined. Fig 4(a) shows the absorption of Pb^{2+}metal ion elimination increased greatly when pH climbed from 3 to 4 and remained steady from 4.0 to 5.50. Due to the breakdown of the crystalline structure, the elimination of Pb^{2+} by LDH decreased at lowering pH less than 3 which related to the competition between the positive proton and the Pb^{2+} metal ions. However, the increasing in pH level, these surface-active sites become higher negatively charged which reduces the competition between positive charges and improves the adsorption of positive Pb^{2+} through the electrostatic force attraction. From the investigated zeta potential of the prepared material at Table 2 we can concluded that beyond pH 3 the absorptivity enhanced due to electrostatic attraction between negative partials of adsorbent and Pb^{2+}.

Table 2. At various pH levels, the Zn/Mg/Fe LDH's Zeta potential (mv), particle size (nm), and percent of removal.

pH	Zeta potential (mv)	Particle size (nm)	Removal efficiency (%)
3	26	301	50
4	-10.20	293	99.7
5	-13.20	267	99.9
6	-17.00	306	99.6

3.5.2. Effect of starting adsorbent dose

The results obtained throughout the elimination of lead metal ions in relation to the produced LDH quantity ranged from 0.01 to 0.07g for 20.0 ml of 50 ppm Pb^{2+}solution at pH=5 for 24 hours is represented in (Figure 4(b)). The results of the removed Pb^{2+} said that by increasing adsorbent dosage the Pb^{2+} removal rate increases too, and the highest value is obtained at 0.05 gm, the efficiency of the adsorption process had increased by the increase in the initial dose of the created LDH nanomaterial, and this could be due to the great number of active sites, the best dose was 0.05, but by increasing the initial dose, the efficiency became fixed and no growth in efficiency was detected. This could be a result to the saturation of active sites and strong particle-particle repulsions[40] which probably matched with the particle size results, Table (2). The hydrodynamic size of a particle indicates how it flows in a fluid. Since the sliding level explains how particles interact with one another, the observed

Preprints (www.preprints.org) | NOT PEER-REVIEWED | Posted: 19 October 2023 doi:10.20944/preprints202310.1287.v1

hydrodynamic (DLS) diameter of the nanomaterial was predicted to be bigger than the partial size determined by SEM. The particle translational diffusion coefficient was affected not only by particle size "core," but also by surface structure, which influences diffusion speed, ion species in the medium, and concentration. Smaller hydrodynamic-sized LDHs nanomaterials have greater aquatic stability than bigger ones, implying a greater potential for long-term usage as an adsorbent for removing contaminants from aquatic mediums. This is a critical consideration for the environmental usage of Zn/Mg/Fe LDH that has various particle sizes (Table 2).

Figure 4. effect of pH on adsorption process (a) and the effect of dose of adsorbent on adsorption process (b)..

3.5.3. Adsorption isotherm study

The success rate of lead ion elimination was investigated experimentally at various starting concentrations of lead ions (from 5-1000 ppm) using a 0.05 g starting dose of LDH material and 20 ml of solution with pH=5 and shackling at 200 rpm for 24 hours. The results obtained indicate that lead removal was greater within the first few values of starting concentrations. However, raising the initial concentration reduced efficiency. This is caused by metal ions' failure to engage with the active sites of the adsorbent LDH substance. According to these findings, raising the metal ion concentration makes the location less energetically favorable[37]. Studying the effect of starting metal ion concentration reveals that the best Pb^{+2} adsorption efficiency occurred at low concentrations and that as Pb^{+2} increased, a corresponding fall in the percent removal progressively occurred. It can be clarified as follows: there are more active sites in the adsorbent at low concentrations of Pb^{+2} which decrease with high metal ion concentrations [41].

The experimental results given in Table 3 are fit correlation coefficient from the Longmuir model (R2=0.92) for the Zn/Mg/Fe LDH. By comparing the Zn/Mg/Fe LDH correlation coefficient from the Frundlish model (R2=0.88). This indicated that the lead ion sorption mechanism on Zn/Mg/Fe LDH was a homogeneous sorption Figure 5(a).

Table 3. Isotherm models of the Adsorption process and their adjustable parameters that result from fitting data.

Isotherm model	parameter	value	Isotherm model	parameter	Value
	q_{max}	700		q_{max}	522.49
	K_L	0.082	Dubinin-	k_{ad}	0.0009
Langmuir	R^2	0.92	Radushkevich	R^2	0.97
	K_f	64.44		q_{max}	378.58
	1/nf	0.68		K_s	0.044
Freundlish	R^2	0.88	Sips	1/n	2.44

3.5.4. Time effect on lead ions removal and kinetic study

In this study, the contact time of adsorption was followed. Figure 5(b) shows two steps of the Pb^{+2} sorption on the nanomaterial. At the first step the adsorption process is rapid due to the reactions of the surface (physical and chemical), complexation and electrostatic attraction on the surface of the sorbent. The second step includes a slow reaction and limited adsorption percentage of Pb^{2+} with the progress of contact time. It means that the adsorption starts rapidly and then slowed gradually. When

Preprints (www.preprints.org) | NOT PEER-REVIEWED | Posted: 19 October 2023 doi:10.20944/preprints202310.1287.v1

the sorption sites decrease, on the adsorbent surface, sorption becomes slower due to the decrease in sorption sites [40]. In the first few mints, more than 99% of the $Pb^{2+}$was removed. Next hour the metal ion concentration remained steady, and the residual metal ion concentration did not show a remarkable change.

The adsorption of metal ion molecules onto the surface of the LDH solid phase nanomaterial at optimum pH and the adsorbent dose is described with four kinetic models, pseudo-first-order model, pseudo-second-order model, a mixed first-second order model, and an intramolecular diffusion model, are used to ascertain if the process of the adsorption is chemosorption or physisorption and its mechanism [42]. In addition to the curves derived from the kinetic models, Figure 5 (b) also displays the experimentally provided data. The models and their fitted parameters for the employed kinetic models are shown in Table 4. According to the testing results, Pb^{+2} was removed 90% quickly in the first 5 minutes, slowly over the next 60 minutes with a 92% removal effectiveness, and then remained stable for the next 120 minutes. It is clear from the correlation coefficient R2 that the pseudo-first-order model, with R2=0.998 for the first model, best fits the adsorption results of Zn/Mg/Fe LDH.

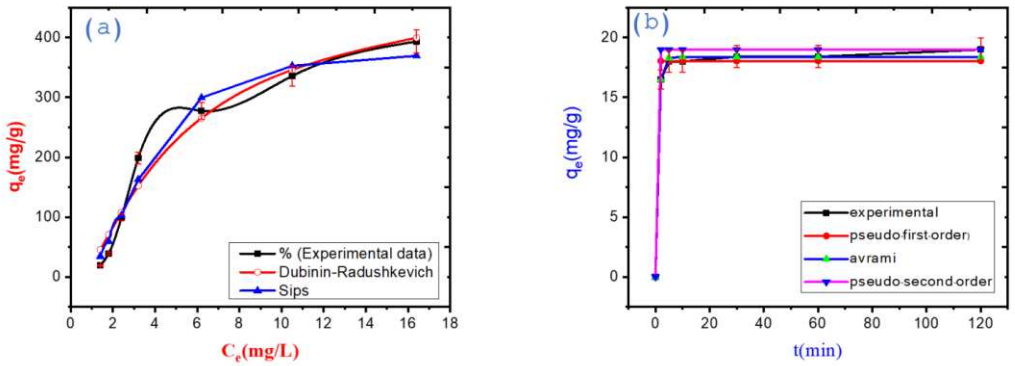

Figure 5. Isotherm data of adsorption process for Pb^{2+} on the created LDH (a) and Kinetic models for solutions of Pb^{2+} metal ions on the Zn/Mg/Fe LDH (b).

Table 4. Coefficients correlations of the models for lead ion adsorption on Zn /Mg /Fe LDH.

Kinetics model	parameter	value	R^2
Pseudo-first order	q_e	18.05	0.998
	k_1	$1.86*10^5$	
Pseudo-sec ond order	q_e	19.00	0.992
	k_2	$1.03*10^6$	
Avarmi	q_e	18.38	0.999
	k_{av}	1.09	

3.5.5. Effect of the Zn/Fe LDH-PANI on A549 and WI-38 Cell Viability

The MTT assay was used to evaluate cell viability following a 48-hour treatment with Zn/Fe LDH-PANI in both A549 and WI-38 cell lines, as depicted in Figure 6(a). In general, the viability of A549 cells significantly decreased as the concentration of Zn/Fe LDH-PANI increased. The IC50% was found to be 80.36 µg/mL, highlighting the strong cytotoxic impact of the Zn/Fe LDH-PANI nanocomposite on A549 cells, which is in line with previous reports[43] Furthermore, when assessing

Preprints (www.preprints.org) | NOT PEER-REVIEWED | Posted: 19 October 2023 doi:10.20944/preprints202310.1287.v1

the safety of the Zn/Fe LDH-PANI nanocomposite on normal cells, particularly WI-38, the outcomes were favorable. The IC50% against WI-38 cells was 200.1 µg/mL, indicating the nanocomposite's outstanding safety profile as an anti-cancer agent. Thus, we established that the Zn/Fe LDH-PANI nanocomposite exhibits anticancer activity against A549 cells by inhibiting their growth. Moreover, we investigated the effects of the Zn/Fe LDH-PANI nanocomposite on the morphology A549 and WI-38. A549 cells were treated with the Zn/Fe LDH-PANI nanocomposite at a concentration of 80.36 µg/mL for 24 hours (Figure 6b). Our results demonstrated a significant alteration in the morphology of the A549 cancer cells. The treatment induced noticeable changes in cell shape and structure, indicating that the nanocomposite has a substantial impact on A549 cells. These observations suggest a potential therapeutic effect of the nanocomposite against A549 cancer cells. In contrast to the significant morphological changes observed in A549 cells, the treatment with the nanocomposite did not affect the morphology of WI-38 cells. This result suggests that the Zn/Fe LDH-PANI nanocomposite is safe for WI-38 normal cell lines, and does not disrupt their cellular structure or integrity.

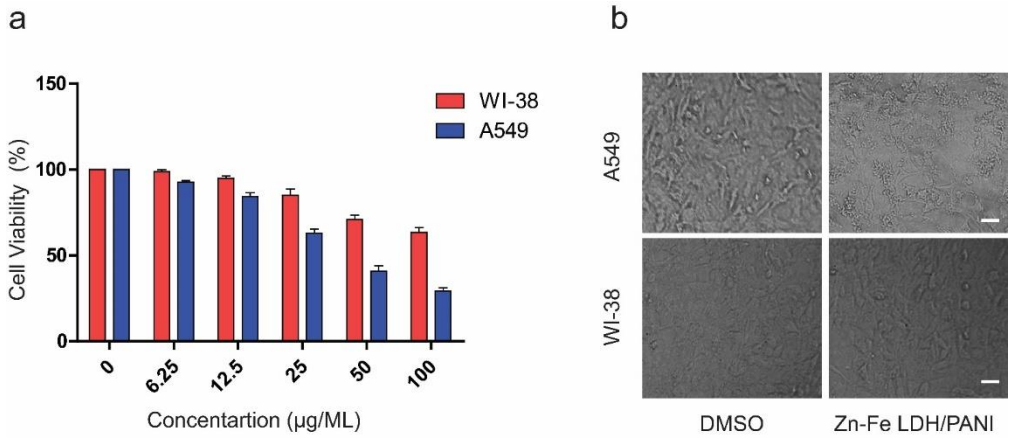

Figure 6. (A) A549 and WI-38 cells were treated with Zn/Fe LDH-PANI (100, 50, 25, 12.5, and 6.25 µg/mL) for 48 hours prior to conducting the MTT assay to estimate cell viability. (b) Morphological changes in A549 and WI-38 cells after Zn/Fe LDH-PANI treatment.

4. Conclusion

The sensing platform upgraded with Zn/Fe LDH-PANI demonstrated a broad linear range of 1-80 M with an achievable limit of determination (LOD) of 167.8 nM and a limit of quantification (LOQ) of 559.4 nM when using DPV for Pb^{+2} detection. In this study, the liquid phase co-precipitation method used to generate the Zn/Mg/Fe LDH nanocomposite and its potential uses in the removal of Pb^{+2} ions are discussed. The ability for lead ion adsorption improves with higher metal ion concentrations and adsorbent amounts. The effectiveness with which lead ions are removed from the aqueous medium depends in large part on the pH of the media. The maximal Zn/Mg/Fe LDH efficiency at pH = 5 after 120 min in the presence of 0.07 gm adsorbent nanomaterial. The pseudo-first-order and Langmuir models were fitted to the adsorption process results. Moreover, our findings indicated that Zn-Fe LDH/PANI reduced cell viability in a dose-dependent manner. Furthermore, Zn-Fe LDH/PANI exhibited a promising safety profile when assessed on WI-38.

Acknowledgment: The authors acknowledge Princess Nourah bint Abdulrahman University Researchers Supporting Project number (PNURSP2023R5), Princess Nourah bint Abdulrahman University, Riyadh, Saudi Arabia

Abbreviations

Heavy metals	HMs

 doi:10.20944/preprints202310.1287.v1

Carbon paste electrode	CPE
Layered double hydroxide	LDH
Polyaniline	PANI
Fourier-transform infrared	FTIR
X-ray diffraction	XRD
Scanning electron microscopy	SEM
Cyclic voltammetry	CV
Differential pulse voltammetry	DPV
Limit of detection	LOD
Limit of quantification	LOQ
Atomic absorption spectrophotometer	AAS
Adsorption capacity	q_m
Double distilled water	DDW

References

1. A. Azmeri, A. Yulianur, U. Zahrati and I. Faudli, Effects of irrigation performance on water balance: Krueng Baro Irrigation Scheme (Aceh-Indonesia) as a case study, *J. Water L. Dev.*, 2019, **42**, 12–20.
2. M. Shafiq, A. A. Alazba and M. T. Amin, *Sains Malaysiana*, 2018, 47, 35–49.
3. Y. L. Xie, S. Q. Zhao, H. L. Ye, J. Yuan, P. Song and S. Q. Hu, Graphene/CeO2 hybrid materials for the simultaneous electrochemical detection of cadmium(II), lead(II), copper(II), and mercury(II), *J. Electroanal. Chem.*, 2015, **757**, 235–242.
4. J. Hur, J. Shin, J. Yoo and Y. S. Seo, Competitive adsorption of metals onto magnetic graphene oxide: Comparison with other carbonaceous adsorbents, *Sci. World J.*, , DOI:10.1155/2015/836287.
5. T. A. Kurniawan, G. Y. S. Chan, W. H. Lo and S. Babel, Physico-chemical treatment techniques for wastewater laden with heavy metals, *Chem. Eng. J.*, 2006, **118**, 83–98.
6. P. N. Omo-Okoro, A. P. Daso and J. O. Okonkwo, *Environ. Technol. Innov.*, 2018, 9, 100–114.
7. Q. Ding, C. Li, H. Wang, C. Xu and H. Kuang, Electrochemical detection of heavy metal ions in water, *Chem. Commun.*, 2021, **57**, 7215–7231.
8. Zirlianngura, D. Tiwari, J. H. Ha and S. M. Lee, Efficient use of porous hybrid materials in a selective detection of lead(II) from aqueous solutions: An electrochemical study, *Metals (Basel).*, , DOI:10.3390/met7040124.
9. C. G. Elinder, L. Friberg, T. Kjellström, G. Nordberg, G. Oberdoerster and W. H. O. O. of G. and I. E. Health, 1994, 78.
10. Z. W. Zhang, S. Shimbo, N. Ochi, M. Eguchi, T. Watanabe, C. S. Moon and M. Ikeda, Determination of lead and cadmium in food and blood by inductively coupled plasma mass spectrometry: A comparison with graphite furnace atomic absorption spectrometry, *Sci. Total Environ.*, 1997, **205**, 179–187.
11. B. Beltrán, L. O. Leal, L. Ferrer and V. Cerdà, Determination of lead by atomic fluorescence spectrometry using an automated extraction/pre-concentration flow system, *J. Anal. At. Spectrom.*, 2015, **30**, 1072–1079.
12. A. Depeursinge, D. Racoceanu, J. Iavindrasana, G. Cohen, A. Platon, P.-A. Poletti and H. Muller, Fusing Visual and Clinical Information for Lung Tissue Classification in HRCT Data, *Artif. Intell. Med.*, 2010, **229**, ARTMED1118.
13. G. A. El-Fatah, H. S. Magar, R. Y. A. Hassan, R. Mahmoud, A. A. Farghali and M. E. M. Hassouna, A novel gallium oxide nanoparticles-based sensor for the simultaneous electrochemical detection of Pb2+, Cd2+ and Hg2+ ions in real water samples, *Sci. Rep.*, 2022, **12**, 1–14.

14. A. Afkhami, H. Ghaedi, T. Madrakian and M. Rezaeivala, Highly sensitive simultaneous electrochemical determination of trace amounts of Pb(II) and Cd(II) using a carbon paste electrode modified with multi-walled carbon nanotubes and a newly synthesized Schiff base, *Electrochim. Acta*, 2013, **89**, 377–386.
15. I. K. Tonlé, S. Letaief, E. Ngameni, A. Walcarius and C. Detellier, Square wave voltammetric determination of lead(II) ions using a carbon paste electrode modified by a thiol-functionalized kaolinite, *Electroanalysis*, 2011, **23**, 245–252.
16. F. Tahernejad-Javazmi, M. Shabani-Nooshabadi and H. Karimi-Maleh, 3D reduced graphene oxide/FeNi3-ionic liquid nanocomposite modified sensor; an electrical synergic effect for development of tert-butylhydroquinone and folic acid sensor, *Compos. Part B Eng.*, 2019, **172**, 666–670.
17. H. Karimi-Maleh, M. Shafieizadeh, M. A. Taher, F. Opoku, E. M. Kiarii, P. P. Govender, S. Ranjbari, M. Rezapour and Y. Orooji, The role of magnetite/graphene oxide nano-composite as a high-efficiency adsorbent for removal of phenazopyridine residues from water samples, an experimental/theoretical investigation, *J. Mol. Liq.*, 2020, **298**, 112040.
18. F. E. Salih, A. Ouarzane and M. El Rhazi, Electrochemical detection of lead (II) at bismuth/Poly(1,8-diaminonaphthalene) modified carbon paste electrode, *Arab. J. Chem.*, 2017, **10**, 596–603.
19. S. Muralikrishna, D. H. Nagaraju, R. G. Balakrishna, W. Surareungchai, T. Ramakrishnappa and A. B. Shivanandareddy, Hydrogels of polyaniline with graphene oxide for highly sensitive electrochemical determination of lead ions, *Anal. Chim. Acta*, 2017, **990**, 67–77.
20. R. Rojas, M. R. Perez, E. M. Erro, P. I. Ortiz, M. A. Ulibarri and C. E. Giacomelli, EDTA modified LDHs as Cu2+ scavengers: Removal kinetics and sorbent stability, *J. Colloid Interface Sci.*, 2009, **331**, 425–431.
21. M. A. Barakat, *Arab. J. Chem.*, 2011, 4, 361–377.
22. A. A. Mohammed and I. S. Samaka, Bentonite coated with magnetite Fe3O4 nanoparticles as a novel adsorbent for copper (II) ions removal from water/wastewater, *Environ. Technol. Innov.*, 2018, **10**, 162–174.
23. A. N., E. A. T., W. D. and D. E. D., Synthesis and Application of Layered Double Hydroxide for the removal of Copper in Wastewater, *Int. J. Chem.*, 2015, **7**, 122.
24. P. Taylor, Y. Yasin, M. Mohamad, A. Saad, A. Sanusi and F. H. Ahmad, Desalination and Water Treatment Removal of lead ions from aqueous solutions using intercalated tartrate-Mg – Al layered double hydroxides, 37–41.
25. M. S. Mostafa, A. A. Bakr, A. M. A. El Naggar and E. A. Sultan, Journal of Colloid and Interface Science Water decontamination via the removal of Pb (II) using a new generation of highly energetic surface nano-material : Co + 2 Mo + 6 LDH, *J. Colloid Interface Sci.*, 2016, **461**, 261–272.
26. H. M. Abdul-Hameed and M. F. Al Juboury, MgFe-doubled layers hydroxide intercalated with low cost local adsorbent using for removal of lead from aqueous solution, *J. Water L. Dev.*, 2020, **45**, 10–18.
27. W. Chen, J. Xing, Z. Lu, J. Wang, S. Yu, W. Yao, A. M. Asiri, K. A. Alamry, X. Wang and S. Wang, *Environ. Chem. Lett.*, 2018, 16, 561–567.
28. F. Lyu, H. Yu, T. Hou, L. Yan, X. Zhang and B. Du, Efficient and fast removal of Pb 2+ and Cd 2+ from an aqueous solution using a chitosan/Mg-Al-layered double hydroxide nanocomposite, *J. Colloid Interface Sci.*, 2019, **539**, 184–193.
29. J. Sun, Y. Chen, H. Yu, L. Yan, B. Du and Z. Pei, Removal of Cu2+, Cd2+ and Pb2+ from aqueous solutions by magnetic alginate microsphere based on Fe3O4/MgAl-layered double hydroxide, *J. Colloid Interface Sci.*, 2018, **532**, 474–484.
30. G. Huang, D. Wang, S. Ma, J. Chen, L. Jiang and P. Wang, A new, low-cost adsorbent: Preparation, characterization, and adsorption behavior of Pb(II) and Cu(II), *J. Colloid Interface Sci.*, 2015, **445**, 294–302.
31. N. K. Gupta, M. Saifuddin, S. Kim and K. S. Kim, Microscopic, spectroscopic, and experimental approach towards understanding the phosphate adsorption onto Zn–Fe layered double hydroxide, *J. Mol. Liq.*, , DOI:10.1016/j.molliq.2019.111935.
32. A. A. H. Faisal, S. F. A. Al-wakel, H. A. Assi, L. A. Naji and M. Naushad, Journal of Water Process Engineering Waterworks sludge- fi lter sand permeable reactive barrier for removal of toxic lead ions from contaminated groundwater, *J. Water Process Eng.*, 2020, **33**, 101112.
33. K. S. Hashim, P. Kot, S. L. Zubaidi, R. Alwash, A. Shaw, D. Al-jumeily and M. H. Aljefery, Energy e ffi cient electrocoagulation using ba ffl e-plates electrodes for e ffi cient Escherichia coli removal from wastewater, 2020, **33**, 1–7.
34. K. S. Hashim, R. Al Khaddar, N. Jasim, A. Shaw, D. Phipps, P. Kot, M. O. Pedrola, A. W. Alattabi, M. Abdulredha and R. Alawsh, Electrocoagulation as a green technology for phosphate removal from river water, *Sep. Purif. Technol.*, 2019, **210**, 135–144.
35. R. K. Mahmoud, A. A. Kotp, A. G. El-Deen, A. A. Farghali and F. I. Abo El-Ela, Novel and Effective Zn-Al-GA LDH Anchored on Nanofibers for High-Performance Heavy Metal Removal and Organic Decontamination: Bioremediation Approach, *Water. Air. Soil Pollut.*, , DOI:10.1007/s11270-020-04629-4.
36. U. Holzwarth and N. Gibson, The Scherrer equation versus the ' Debye – Scherrer equation ', 2011, **6**, 21027.
37. M. Alkan, B. Kalay, M. Doğan and Ö. Demirbaş, *J. Hazard. Mater.*, 2008, 153, 867–876.

38. O. G. Hussein, K. Abdou, W. A. Moselhy and R. Mahmoud, Applied Clay Science high-efficiency removal of copper metal ions . The experimental , possible mechanism , sustainable use of waste , and safety study, *Appl. Clay Sci.*, 2023, **231**, 106724.
39. H. A. Younes, R. Khaled, H. M. Mahmoud, H. F. Nassar, M. M. Abdelrahman, F. I. Abo El-Ela and M. Taha, Computational and experimental studies on the efficient removal of diclofenac from water using ZnFe-layered double hydroxide as an environmentally benign absorbent, *J. Taiwan Inst. Chem. Eng.*, 2019, **102**, 297–311.
40. B. M. W. P. K. Amarasinghe and R. A. Williams, Tea waste as a low cost adsorbent for the removal of Cu and Pb from wastewater, *Chem. Eng. J.*, 2007, **132**, 299–309.
41. M. J. Barnabas, S. Parambadath, A. Mathew, S. S. Park, A. Vinu and C. S. Ha, Highly efficient and selective adsorption of In3+ on pristine Zn/Al layered double hydroxide (Zn/Al-LDH) from aqueous solutions, *J. Solid State Chem.*, 2016, **233**, 133–142.
42. M. C. Alexandrica, M. Silion, D. Hritcu and M. I. Popa, Layered Double Hydroxides As Adsorbents for Anionic Dye Removal From Aqueous Solutions, *Environ. Eng. Manag. J.*, 2018, **14**, 381–388.
43. Saranya, J., et al. "Microwave thermally assisted porous structured cerium oxide/zinc oxide design: fabrication, electrochemical activity towards Pb Ions, anticancer assessment in HeLa and VERO cell lines." *Journal of Inorganic and Organometallic Polymers and Materials* 31 (2021): 1279-1292.